INFUENCE OF UNCERTAIN VERTICAL LOADS AND ACCELERATIONS ON THE SEISMIC PERFORMANCE OF AN RC BUILDING[1]

Dimitrios Vamvatsikos, Dept. of Civil & Env. Engineering, Univ. of Cyprus, Cyprus
Christos Zeris, School of Civil Engineering, NTU Athens, Greece

ABSTRACT

We investigate the influence of the uncertain value of the gravity loads and the vertical ground motion component on the seismic performance of a non-ductile reinforced concrete building. Seismic guidelines typically enforce the use of the $G_\kappa + 0.3Q_\kappa$ combination, where G_κ, Q_κ are the characteristic dead and live loads, respectively. However, their true values and their influence to the seismic response are not known. Using a typical existing five-story reinforced concrete building, we employ incremental dynamic analysis to evaluate the seismic performance under probabilistic load distributions in combination with the use or not of the vertical component of ground motion. Multiple accelerograms are scaled to several levels of intensity, both in the horizontal and in the vertical sense, to evaluate the building capacity in limit-states ranging from serviceability to global dynamic instability and structural collapse. Thus, it is shown that the highly variable live loads tend to increase the response uncertainty especially when they dominate over dead loads. On the other hand, the effect of vertical accelerations depends on the magnitude of the gravity loads, with higher loads causing significant capacity reductions across all limit-states considered.

Keywords: Earthquake, Vertical acceleration, Incremental dynamic analysis, Static pushover, Uncertainty, Reinforced concrete.

[1] Based on a short paper presented at the 3rd Panhellenic Conference on Earthquake Engineering and Engineering Seismology, Athens, 2008 (in Greek).

INTRODUCTION

According to modern seismic design provisions (e.g., GSC[1] and EC8[2]) the mass and the corresponding gravity loads considered in the seismic load combinations amount to 100% of the dead loads plus 30% of the live loads for typical residential buildings. Obviously, the actual value at the time of the earthquake is uncertain and it could be either lower or higher than the designated one. Additionally, the issue of the vertical seismic component — which is allowed to be ignored in the design of regular buildings of normal importance and in low to medium seismicity areas — is another major unknown, as its influence in the structural response is not yet clear, nor is it well understood how safe it is to assume that it can be ignored.

Both issues have been of considerable research interest in the past. The sensitivity of the seismic behavior of structures to changes in their mass has been studied, at least for steel frames, by Al-Ali & Krawinkler[3] and Fragiadakis et al[4]. Although the original purpose was to estimate the influence of story-level changes in mass, the results show a relatively medium to low influence of seismic masses to the building response, especially when compared to the influence of other building parameters (e.g. the flexural resistance of the beam plastic hinges). Still, the potential influence of the gravity load intensity to the strength and stiffness of the structural elements, an issue of importance particularly for reinforced concrete (RC) members, was not taken into account, as lumped-plasticity elements were used with predefined moment-rotation relationships and constant stiffness in the plastic hinges.

Several studies have also appeared, investigating the influence of the vertical seismic acceleration on the structural response. Nevertheless, the results point both ways. For example, Chopra[5] found a significant effect of vertical accelerations on the stresses appearing in gravity dams, while Munshi and Ghosh[6] observed little influence on the response of a modern RC building. On the other hand, Papazoglou and Elnashai[7] offer significant evidence for potential collapses due to vertical ground motion excitation in recent earthquakes, while they employ structural analyses to point to the associated high-frequency, high-amplitude variation in the axial load of columns. Still, most existing studies are mainly focused on assessing the changes caused by vertical accelerations to internal stresses, forces or moments, without investigating the influence of such changes to the actual seismic performance. In essence, what is lacking is a quantitative (and not just qualitative) evaluation of the influence of vertical loads and accelerations to the actual seismic performance of RC structures.

METHODOLOGY

In order to provide a comprehensive answer to this complex issue we propose the use of incremental dynamic analysis (IDA, Vamvatsikos and Cornell[8]) to estimate the seismic performance of structures under varying loading conditions. IDA is nowadays an established methodology that allows the accurate assessment of the seismic demand and capacity of structures. Using numerous nonlinear dynamic analyses under multiply scaled ground motion records, it forces the structure through the entire range of response and through all limit-

states, from serviceability to global dynamic instability. It is a computationally-intensive method which, however, offers a complete picture of the seismic performance of structures while allowing for a detailed comparison of structural response and capacity under different modeling and design assumptions without the shortcomings of static response prediction.

The results of IDA appear in terms of the Intensity Measure (IM) of the earthquake, i.e., a scalar measure that represents the scaling of each ground motion record, versus the resulting Engineering Demand Parameter (EDP) value which stands for the structural response. Typically, the 5%-damped first-mode spectral acceleration, $S_a(T_1,5\%)$ is used as the IM, while the maximum (over all stories) peak interstory drift, $\theta_{\max}$ serves as a possible candidate for the EDP. By appropriately interpolating such IM-EDP pairs, continuous IDA curves are generated, one for each ground motion record. These are in turn summarized to their 16, 50 και 84% fractile curves (Vamvatsikos and Cornell[8]), offering a complete description of the (central value and dispersion of the) distribution of the structural response and capacity.

Thus, we created Figs 1a and 1b where we have subjected a typical existing five-story RC building to multiple ground motion records without and with the corresponding vertical acceleration component, respectively. Therein we observe that all IDA curves terminate in a flatline where the IM reaches its maximum value, which differs for each record. This flatline is where the building reaches global dynamic instability, thus being unable to sustain higher base excitation intensities. In essence, these maximal values of $S_a(T_1,5\%)$ characterize the collapse capacity of the building, in the same way that the derived $S_a(T_1,5\%)$-value for any other limit-state will uniquely characterize it. By comparing the two figures we can immediately distinguish the differences in $S_a(T_1,5\%)$ capacity caused by the inclusion of the vertical component for any given value of $\theta_{\max}$. For some records, the vertical ground motion seems to be detrimental, while for others it is clearly beneficial, directly providing some insight into the reasons behind the differing opinions that have appeared in the literature. In the course of this study, we will investigate this building in detail, using IDA as our mainstay.

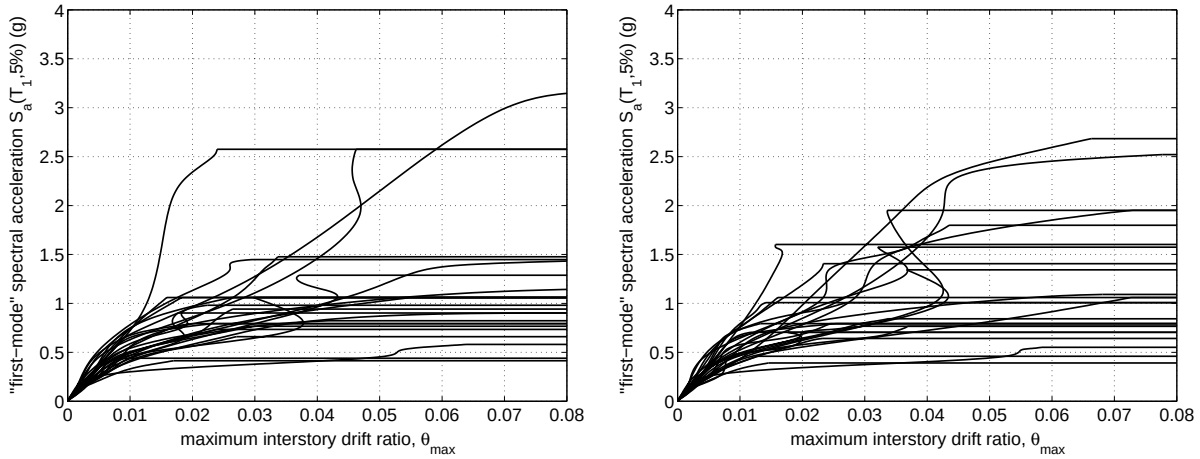

(a) (b)

Fig. 1 IDA curves: (a) without influence; and (b) with influence of the vertical ground motion component, for 100% of the vertical loads according to EC8[2].

GROUND MOTION RECORDS

A suite of 26 ground motion records was employed for the dynamic analyses, each having two components: One of the two horizontal (randomly selected) and the vertical; consequently, only plane frame response is considered, so as not to complicate the problem investigated. In essence these are "ordinary" records devoid of any directivity or soft soil effects. The moment magnitude ranges within 6.5 – 6.9 while the closest distance is 13 – 32km. Due to the relatively low to medium distance from the fault line, the records exhibit vertical accelerations that show a considerable spread, some being significant while others relatively low. Thus, the ratio of Peak Vertical Acceleration (PVA) to Peak Horizontal Acceleration (PHA) ranges from 0.2 up to 2.3, while 10 out of 26 (i.e., the 39%) show ratios higher than the typically assumed 2/3 (Newmark et al[9]), let alone 1/3, typically specified in design (when required). In other words, these records display a wide variety of characteristics, as seen in detail in Table 1.

Table 1 The suite of ground motion records used.

Event Station	R [a] (km)	Soil [b]	Φ [c] (deg)	PHA [d] (g)	PVA [e] (g)	PVA/PHA (g)
Superstition Hills 1987 (M=6.7) [f]						
1. Wildlife Liquef. Array	24.4	–,D	090	0.18	0.41	2.28
2. Westmoreland Fire Station	13.3	C,D	090	0.17	0.25	1.47
3. El Centro Imp. Co Cent	13.9	C,D	000	0.36	0.13	0.36
San Fernando, 1971 (M=6.6)						
4. LA Hollywood Sto Lot	21.2	C,D	090	0.21	0.14	0.67
Imperial Valley 1979 (M=6.5)						
5. Plaster City	31.7	C,D	045	0.04	0.03	0.75
6. El centro Array #12	18.2	C,D	140	0.14	0.07	0.50
7. El centro Array #13	21.9	C,D	140	0.12	0.05	0.42
8. Westmoreland Fire Station	15.1	C,D	090	0.07	0.08	1.14
9. El centro Array #1	15.5	C,D	140	0.14	0.06	0.43
Northridge 1994 (M=6.7)						
10. Leona Valley #2	37.7	C,–	000	0.09	0.06	0.67
11. Lake Hughes #1	36.3	C,C	000	0.09	0.10	1.11
12. LA Hollywood Sto FF	25.5	C,D	090	0.23	0.14	0.61
13. LA Baldwin Hills	31.3	B,B	090	0.24	0.09	0.38
14. Canoga Park - Topanga Can	15.8	C,D	106	0.36	0.49	1.36
15. LA N Faring Rd	23.9	C,B	000	0.27	0.19	0.70
16. LA Fletcher Dr	29.5	C,D	144	0.16	0.11	0.69
17. LA Centinela St	30.9	C,D	155	0.47	0.11	0.23
18. Glendale Las Palmas	25.4	C,C	177	0.36	0.13	0.36
Loma Prieta 1989 (M=6.9)						
19. Hollister Diff Array	25.8	–,D	165	0.27	0.15	0.56
20. WAHO	16.9	–,D	000	0.37	0.27	0.73
21. Halls Valley	31.6	C,C	000	0.13	0.06	0.46
22. Agnews State Hospital	28.2	C,D	000	0.17	0.09	0.53
23. Anderson Dam Downstrm	21.4	B,D	270	0.24	0.15	0.63
24. Coyote Lake Dam Downstrm	22.3	B,D	195	0.16	0.10	0.63
25. Sunnyvale Colton Ave	28.8	C,D	270	0.21	0.10	0.48
26. Hollister South & Pine	28.8	–,D	000	0.37	0.20	0.54

[a] Closest distance to fault

[b] USGS, Geomatrix soil category
[c] Direction of horizontal component
[d] Peak horizontal ground acceleration
[e] Peak vertical ground acceleration
[f] Moment magnitude

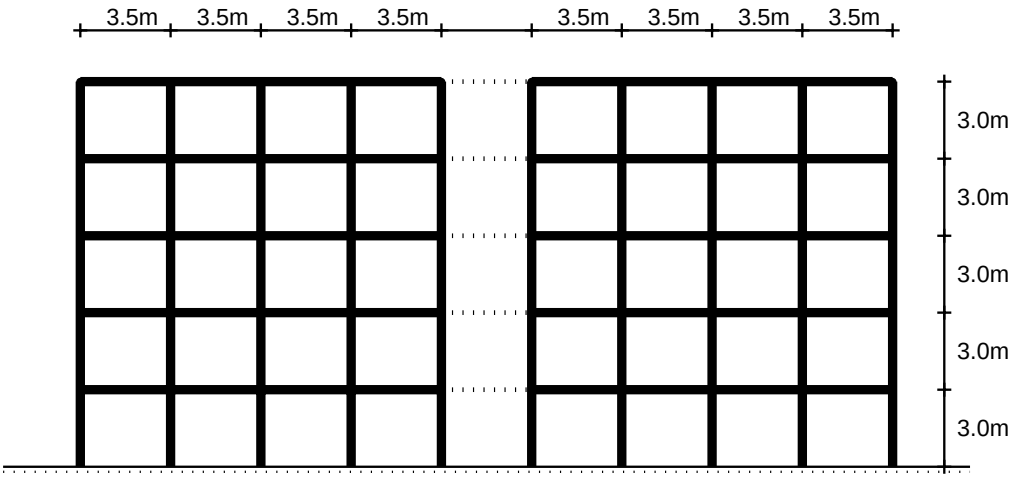

Fig. 2 The 2D model of the five-story RC building..

BUILDING AND STRUCTURAL MODEL

The building to be analyzed is a typical non-conforming five-story RC structure, representative of the design and construction practices of the 1960's in several moderate seismicity areas. The plan is symmetric, four by three bays and each of the five stories is 3.00m high (Zeris et al[10]). It has been designed using allowable stresses for moderate seismic forces according to the Greek Seismic Code of 1959 (RD59[11]), taking into account the geometric properties, materials and design loads of the era it represents (Repapis et al[12]).

It is modeled as a two-dimensional, four-bay plane frame in the longitudinal direction. Due to symmetry, it is adequate to model only half of the structure, using just one external and one internal frame placed in parallel in 2D (Zeris et al[10]) and rigidly connected to each other at each floor level due to the existence of the diaphragm (Fig. 2). Using the OpenSees analysis platform (McKenna et al[13]) we have modeled the beams and columns with force-based, distributed damage elements. All members are monitored in control sections at the ends and within the member, all sections being properly discretized into concrete and steel fibers. The slab reinforcement is taken into account within the effective width to estimate the response of the beams under negative bending moments, assuming different effective widths for the internal and external frame beams (1.0m and 0.5m respectively). The uniaxial stress-strain curves of the fibers are based on the mean, rather than the characteristic, properties of the corresponding materials. The mean strength of unconfined concrete is taken to be 18MPa for grade C16 (B120), while the effect of confinement (although quite low due to the large stirrup spacing) is taken into account according to Mander et al[14]. For the longitudinal

reinforcement, based on actual experiments with smooth 14mm rebars, we have used a mean yield stress of 310MPa and bilinear characteristics. To achieve an accurate representation of the varying reinforcement along each beam, and to capture the exact initial distribution of moments due to gravity loads, each beam has been uniformly subdivided into five beam-column elements with five control sections per element. On the other hand, columns are modeled as only one, five-section beam-column element that includes a first order treatment of geometric nonlinearities (P-Δ effects).

The design gravity loads used are: a) the building self-weight that includes a 25cm-wide perimeter clay brick infill wall, b) a 2.50 kN/m^2 uniform load, which (according to code provisions) includes a 1.00 kN/m^2 surcharge for the internal moveable 10cm-wide clay brick partitions and c) the 2.00kN/m^2 live load, typical for residential buildings. The final result is a relatively high-frequency structure with a first mode period of T_1 = 0.57sec and a normalized column axial load that ranges between 0.10 and 0.18 at the ground level.

PROBABILISTIC DISTRIBUTION OF VERTICAL LOADS

For an accurate analysis of the influence of the gravity loads on the structure we need to estimate their actual probabilistic distribution. To this end we will use the load distribution that is implied by the provisions of EC8[2]. According to our data, the building is subject to a characteristic dead load G_κ = 5.38kN/m^2 and a characteristic live load Q_κ = 2kN/m^2. The gravity load considered during seismic excitation (the infrequent event) is defined as $P = G_\kappa + 0.3Q_\kappa$. On the other hand, for pure gravity load analysis, the ultimate value considered uses the higher load partial safety factors γ_f, namely γ_g = 1.35 and γ_q = 1.50 for dead and live loads, respectively. These are meant to set the corresponding loads to their characteristic values that have only a 5% probability of exceedance for non-accidental loading combinations. It should be noted at this point, that we do not apply any statistical variation on the material partial factors γ_m, which retail their code specified value.

According to these assumptions we shall attempt to reconstruct the probabilistic distributions of the load factors so that they are compatible with the above code provisions. Thus, we assume that the dead load partial factor γ_g follows a normal distribution with a mean (or median) of 1.0 and a standard deviation of 0.21 so that its 95% value is 1.35. Similarly, we assume that the live load factor γ_q follows a lognormal distribution with a median of 0.3 and a standard deviation of the logs equal to 0.98 making its 95% value equal to 1.50.

Using a simple Monte Carlo simulation we can easily estimate the distribution of the derived load combination factor γ_p which represents the variability of the combined dead and live load P around its assumed characteristic value of $G_\kappa + 0.3Q_\kappa$:

$$\gamma_p = \frac{\gamma_g G_k + \gamma_q Q_k}{G_k + 0.3Q_k} \quad (1)$$

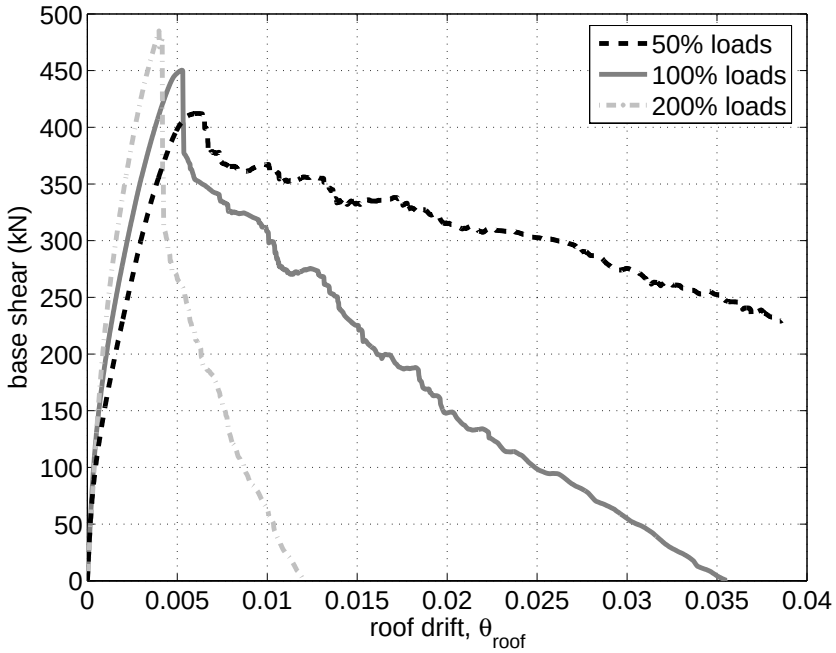

Fig. 3 Static pushover curves for the 50%, 100% και 200% value of the vertical loads.

In our example, the result is a distribution that looks like a normal but still retains a heavy tail on the right showing a propensity to generate relatively higher values of γ_ρ. The actual mean value is 1.06 and the standard deviation 0.28, thus γ_ρ has inherited the characteristics of the normal distribution of the dead loads, something that should be expected, as they do have the largest contribution to the total load P for the building studied. We also observe that the γ_p values with only a 0.5% probability of not being or being exceeded (i.e. the 0.5% and 99.5% percentiles) are approximately 0.5 and 2.0, respectively. These are the two extreme values for the load factor γ_p that will be used to study the sensitivity of structural performance to extreme changes in the gravity loads. In any case, we will assume a uniform load factor across the entire building, thus neglecting any spatial variability.

SENSITIVITY TO VERTICAL LOAD MAGNITUDE

To fully understand the effect of γ_p on the structural behavior, we have performed static pushover analyses for the low, central and high values of 50%, 100% and 200% of P. The resulting pushover curves (Fig. 3) offer a clear picture of the influence of gravity loads on the structure. First of all, we see that increasing the vertical load factor provides the structure with higher initial stiffness while it allows the building to reach a higher maximum base shear. The reason is the higher initial axial load of the columns, closer to their balance load value that allows them to withstand larger bending moments with increased lateral stiffness due to the relatively reduced cracked area, at the cost of a reduced ductility supply, reaching values less than unity above balance. Consequently, under increasing lateral loads, the higher axial load consumes their strength very quickly, leading to a rapid post-peak drop in the pushover curve resulting to reduced overall system ductility. In essence, the increased axial

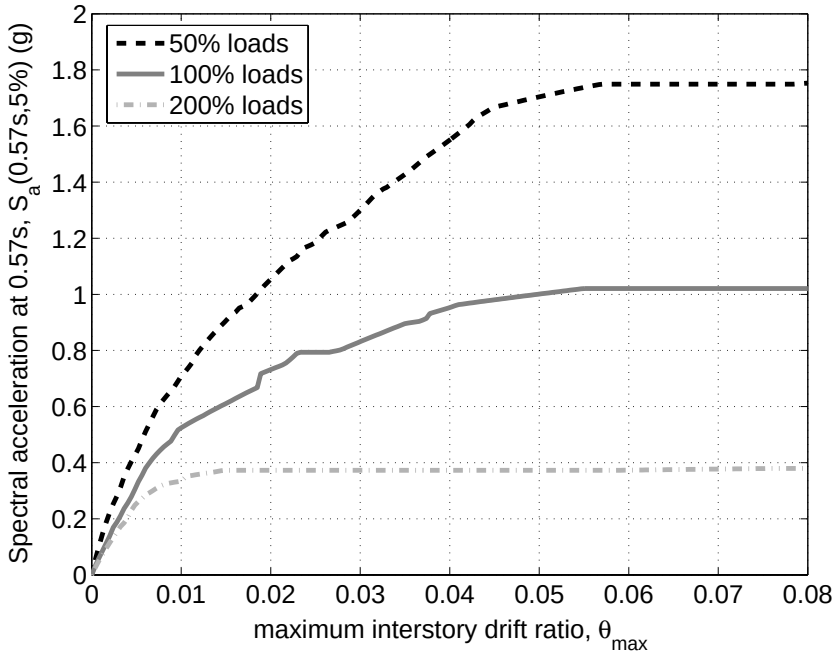

Fig. 4 Median IDA curves for 50%, 100% και 200% of the nominal gravity loads.

load is causing the reduction of local ductilities in the columns, which are critical for this non capacity-designed building. In total, the effects of increasing gravity loads are clearly detrimental: When γ_p increases from 0.5 to 2.0 we have an increase in the maximum base shear of about 20% but a corresponding decrease in the maximum roof drift θ_{roof} by at least a factor of six.

To evaluate the influence of γ_p on the dynamic behavior of the structure we have also performed IDA for each of the three discrete load factor values and extracted the median IDA curves (Vamvatsikos & Cornell[15]). To offset the fact that the mass change also changes the period of the structure, we have used S_a(0.57sec,5%) as a common IM for all three cases, where 0.57s is the first-mode period of the building for γ_p = 1.0 (Fig. 4).

Now, there are two effects working against each other. The first is the increase of the axial loads and the resulting higher stiffness and lower system ductility that we observed in the pushover curves. The second is the influence of the mass change and the corresponding period on the actual seismic loads attracted by the building. In general the value of γ_p = 0.5 corresponds to a low period of T_1 = 0.39sec, which moves the structure to the more aggressive part of the mean spectrum, subjecting it to higher accelerations. On the contrary, the higher value γ_p = 2.0 increases the period to T_1 = 0.92sec and correspondingly reduces the spectral acceleration (but not necessarily the seismic loads as the mass increases). As shown in Fig. 4, this is not enough to balance the rapidly decreasing strength and ductility of the structure caused by the high axial loads. Thus, the IDA curves follow similar trends as the corresponding pushover curves and they are highly influenced by the load factor γ_p: Doubling or halving the nominal gravity loads leads to a corresponding decrease or increase, respectively, of the seismic capacity in S_a(0.57s,5%)-terms in the order of 40 – 60% for any post-elastic limit-state.

UNCERTAINTY DUE TO VERTICAL LOAD VARIABILITY

The sensitivity analyses presented let us comprehend the influence of the load factor qualitatively, but the actual values shown are only indicative of extreme values of γ_p. To obtain an accurate picture of the actual influence of the load factor and its corresponding epistemic uncertainty, we need to take into account its full probabilistic distribution.

In order to assess the mean and standard deviation of the, now uncertain, median IDA curves we employ the first-order second-moment method (FOSM, e.g., Benjamin & Cornell[16]). It is a simple technique that offers relatively accurate results without the need for time-consuming Monte Carlo simulations. The results appear in Fig. 5, where the mean "median IDA curve" appears together with the "median IDA curves" on each side that are one standard deviation apart. These curves accurately represent the central value and the dispersion of the seismic demand and capacity of the structure due to gravity load uncertainties. As also shown in Fig. 6, the effect of the uncertainty on the seismic capacity in IM-terms results in a coefficient of variation of only 6 – 12%; such a low value is indicative of the low participation of the highly variable live-loads in the total gravity loading. Since this is a typical residential RC building, it is to be expected that the dead loads will dominate and they will considerably dampen the influence of the large dispersion of live loads. Compared to the much larger 40% – 50% dispersion observed in Figs 1a-b due to record-to-record variability, we surmise that the gravity load uncertainty can be safely ignored for this particular structure.

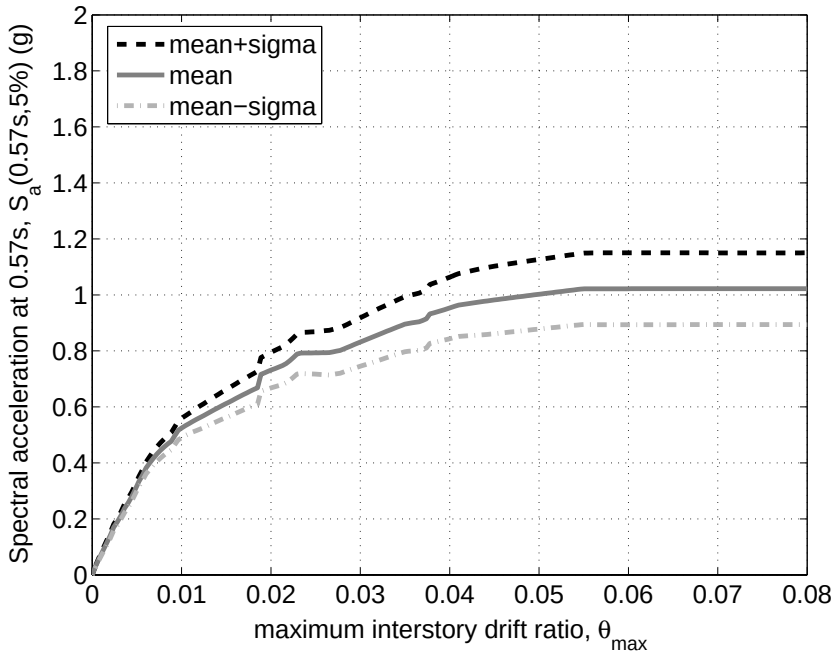

Fig. 5 Variability of the median IDA curves and of the corresponding seismic capacity in S_a(0.57s, 5%)-terms for uncertain gravity loads.

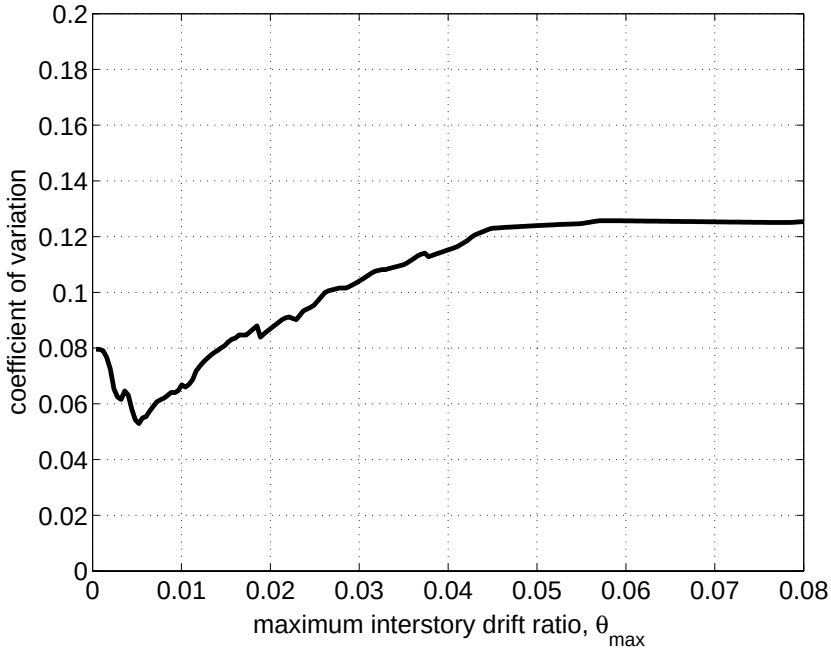

Fig 6 Coefficient of variation of the seismic capacity in S_a(0.57s, 5%)-terms due to uncertain gravity loads.

INFLUENCE OF VERTICAL ACCELERATION

As initially observed in Fig. 1, the inclusion or non-inclusion of the vertical ground motion component in the analysis does influence the estimated building behavior. The question is whether this choice is conservative, i.e., whether it works against or in favor of the actual structural safety and to what degree this is influenced by the gravity loads acting on the structure.

To form a comprehensive answer we performed IDA analyses of the structure having a load factor γ_p = 0.5, 1.0 and 2.0, subjecting it to both the horizontal and vertical ground motion components of each record. The median IDA curves including the influence of vertical accelerations appear in Fig. 7b, where they can be compared to the median IDA curves without vertical accelerations derived earlier and appearing again in Fig. 7a. Using S_a(0.57s,5%) as the common IM we can estimate accurately the differences between the two cases. In general, we observe that the median IDA curves for any given value of γ_p are comparable: There are changes in the S_a(0.57s,5%)-capacity for given $\theta_{\max}$ which vary in magnitude and direction, depending on the limit-state (or value of $\theta_{\max}$) considered.

Using the common IM as a basis we can obtain an immediate qualitative comparison of the results. Thus, Fig. 8 shows the relative change in the estimated S_a(0.57s,5%)-capacity due to the inclusion of the vertical ground motion component for any given value of $\theta_{\max}$. This is naturally defined as the ratio $(S_a^{xz} - S_a^{x})/ S_a^{x}$, where S_a^{x} designates the IM value for horizontal excitation only and S_a^{xz} defines the value for concurrent horizontal and vertical acceleration.

Clearly, for 50% lower gravity loads, the vertical component may often have beneficiary influence that reaches up to a 30% increase in the IM-value of capacity for the lower values of θ_{max}. The increase of the load factor to 100% of its nominal value corresponds to a drastic decrease of such benefits, since the effect of the vertical acceleration seems to be practically zero on average across all values of θ_{max}. When we increase the gravity loads to 200%, then the addition of the vertical excitation is obviously detrimental and it lowers the estimated seismic capacity by almost 10%, often reaching up to 20% drops for certain limit-states.

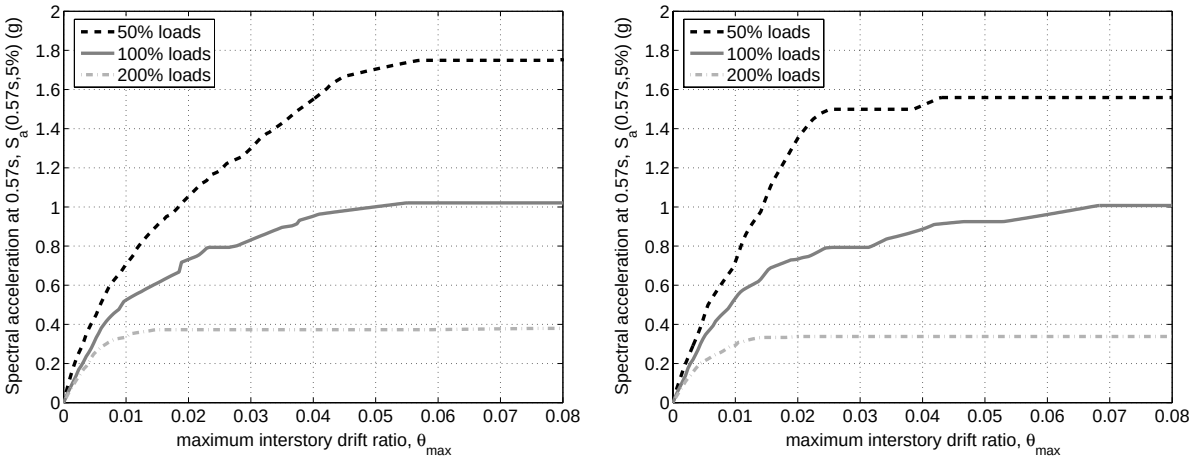

Fig. 7 Median IDA curves (a) excluding and (b) including the vertical ground motion component for 50%, 100% and 200% of the nominal gravity loads.

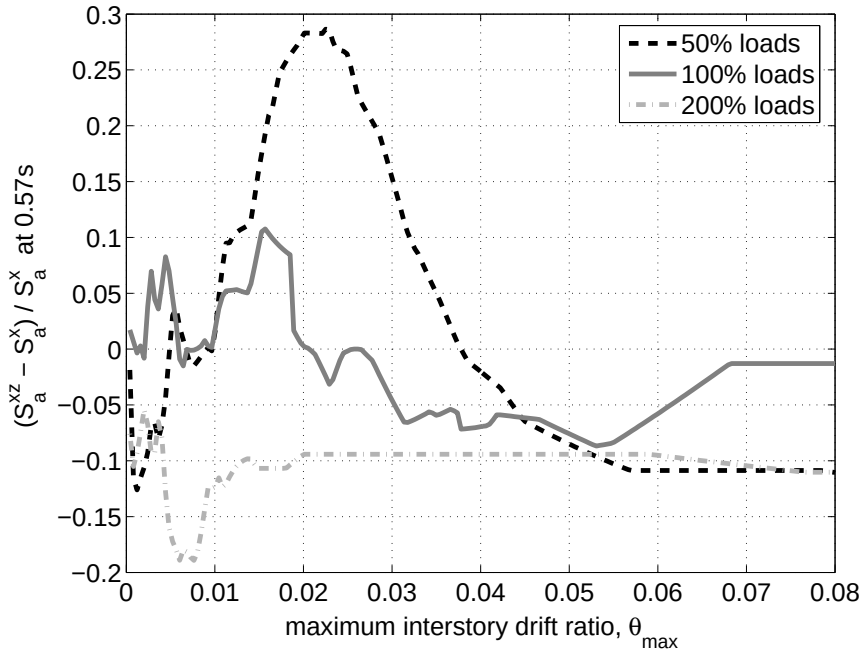

Fig. 8 The relative change $(S_a^{xz} - S_a^x)/ S_a^x$ in the estimated value of the median capacity in S_a(0.57, 5%) terms, when the vertical ground motion component is taken into account, for 50%, 100% and 200% of the characteristic gravity loads.

Therefore, we can observe that there is a decisive difference for the structure when it carries a lower or a larger percentage of its design gravity load, or correspondingly, when the columns carry a lower or a higher normalized axial load. We should keep in mind here that the building has not been capacity-designed; plastic hinges tend to appear in the columns rather than at the beam ends. Thus, any increase in the column axial load has an immediate effect on the stiffness, plastic moment and ductility that the critical column sections can bear, a fact that plays an important role in causing the phenomena appearing in Fig. 8.

It is also important to note that the increase or decrease of the seismic capacity for any given γ_p, when vertical accelerations are included, is not significantly correlated on a record-by-record basis with either the PVA/PHA ratio, the PVA value or the corresponding change for any other value of γ_p. In other words, there is no simple rule to help us predict how, for a given record, the inclusion of the vertical component will affect the structure. The only thing that can be claimed with significant statistical evidence, for this type of structures, is that the relatively higher values of gravity loads have a negative influence on average, while for relatively lower values the effect appears to be random, sometimes positive and other times negative. Consequently, changes in occupancy usage common in such types of buildings, which result in increased gravity loads towards the high end of the distribution, fall under the former case and should be identified for potentially higher seismic vulnerability.

CONCLUSIONS

We have performed static pushover and incremental dynamic analyses in order to quantify the effect of the uncertain gravity loads and the vertical ground motion component on the seismic performance of a typical RC building constructed in the 1960's. We observed that when the dead loads dominate, as often happens in such buildings, then the resulting total gravity loads show a low overall variability causing the influence of the corresponding uncertainties to remain relatively low. In particular, in the case of the five-story RC building examined, the resulting dispersion in the seismic demand and capacity is of the order of 10% only. On the other hand, sensitivity studies show that in the case of the live loads dominating the total gravity load, their influence could become significantly higher. In the case of structures where there are practically deterministic large changes in the live loads, as for example happens in buildings undergoing change of use (from residential to light commercial storage) or structures that may be filled to capacity during a time of the day only to empty at other times (e.g. storage) then the issue of gravity load uncertainty can be quite significant.

The influence of the vertical component of the ground motion appears to depend directly upon the magnitude of the gravity loads and, therefore, the normalized axial load carried by each column. In the building studied, for low gravity loads we may observe either positive or negative influences on the seismic capacity. When the vertical loads are increased, the inclusion of vertical accelerations becomes systematically detrimental, causing up to a 20% decrease in the seismic capacity. Generalized conclusions should not be made, though, before further investigations are carried out on buildings with different geometric (span width) and loading characteristics (e.g, offices, warehouses or parking structures).

ACKNOWLEDGEMENTS

The help of Mr. C. Alexandropoulos and Mr. P. Giannitsas on modeling the structure is gratefully acknowledged.

REFERENCES

1. GSC, *Greek Seismic Code*, Ministry of Environment, Land and Public Works, Athens, Greece, 2000.
2. CEN, "Eurocode 8 - Design of structures for earthquake resistance, Part 1," *European standard prEN 1998-1*, European Committee for Standardization, Brussels, 2003.
3. Al-Ali A.A.K., Krawinkler H., "Effects of vertical irregularities on seismic behaviour of building structures," *Report No 130*, John A. Blume Earthquake Engineering Center, Stanford University, Stanford, CA, 1998.
4. Fragiadakis M., Vamvatsikos D., and Papadrakakis M., "Evaluation of the influence of vertical irregularities on the seismic performance of a 9-storey steel frame," *Earthquake Engineering and Structural Dynamics,* V. 35, No. 12, 2006, pp. 1489–1509.
5. Chopra A.K., "The importance of the vertical component of earthquake motions," *Bulletin of the Seismological Society of America*, V. 56, No. 5, 1966, pp. 1163–1175.
6. Munshi J.A., and Ghosh S.K., "Analyses of seismic performance of a code designed reinforced concrete building." *Engineering Structures*, V. 20, No. 7, 1998, pp.608–616.
7. Papazoglou A.J., and Elnashai A.S., "Analytical and field evidence of the damaging effect of vertical earthquake ground motion," *Earthquake Engineering and Structural Dynamics*, V. 25, 1996, pp. 1109–1137.
8. Vamvatsikos D., and Cornell C.A., "Incremental dynamic analysis," *Earthquake Engineering and Structural Dynamics*, V. 31, 2002, pp. 491–514.
9. Newmark, N. M., Blume, J. A. and Kapur, K. K., "Seismic design spectra for nuclear power plants," *Journal of the Power Division*. V. 99, 1973, pp. 287-303.
10. Zeris C., Giannitsas P., Alexandropoulos K., and Vamvatsikos D., "Inelastic modeling sensitivity of the predicted seismic performance of an existing RC building," *Proceedings of the 1st European Conference on Earthquake Engineering and Seismology,* Geneva, 2006.
11. RD59, "On the Seismic Code for Structures," *Royal Decree 26/2/59*, Ministry of Public Works, Greece, 1959 (in greek).
12. Repapis K., Vintzeleou E., and C. Zeris, "Evaluation of the Seismic Performance of Existing RC Buildings: I Suggested Methodology," *Journal of Earthquake Engineering*, V. 10, No. 2, 2006, pp. 265-288.
13. McKenna F., and Fenves G.L., *The OpenSees Command Language Manual – V.1.2.*, Pacific Earthquake Engineering Research Centre, University of California, Berkeley, (2001).
14. Mander J.B., Priestley M.J.N., and Park R., "Theoretical stress-strain model for confined concrete," *ASCE Journal of Structural Engineering*, V. 114, No. 8, 1988, pp. 1804–1825.
15. Vamvatsikos D., and Cornell C.A., "Applied Incremental Dynamic Analysis," *Earthquake Spectra*, V. 20, No. 2, .2004, pp. 523–553.
16. Benjamin J.R., and Cornell C.A., *Probability, Statistics, and Decision for Civil Engineers*, McGraw-Hill, New York, 1970.